



Unión Europea
Fondo Europeo
de Desarrollo Regional
"Una manera de hacer Europa"



ASTROMETRIC CALIBRATION OF YEBES ALL-SKY CAMERA

YLARA Project

YLARA-LS-60-I05 (CDT Technical Report 2023-04)

J. C. Rodríguez, A. García Marín, J. A. López Pérez, B. Vaquero Jiménez

Yebes Observatory, IGN-CNIG

Note

This technical report is a slightly expanded version of a short [paper](#) submitted to the 22nd International Workshop on Laser Ranging: J.C.Rodríguez et al, “Astrometric Calibration of All-sky Camera for Aircraft Spotting and Meteor Observations”, 22nd IWLRL, Guadalajara (Spain), Nov 7–11, 2022.

Contact Information:

Observatorio de Yebes
Cerro de la Palera s/n
19141 (Yebes), Guadalajara
Tel.: 949 865 124
Email: jc.rodriguez@oan.es

Acknowledgements

The all-sky camera employed for the work described in this report has been acquired thanks to the YDALGO project financed with Multi regional Operational Programme for Spain 2014-20 ERDF funds.

Table of contents

Acknowledgements.....	iii
Table of contents.....	iv
List of figures.....	vi
Abbreviations.....	vii
Applicable and reference documents.....	viii
Abstract.....	ix
1 Introduction.....	1
2 Implementation.....	2
2.1 Hardware.....	2
2.2 Calibration model.....	2
2.3 Strategy.....	5
3 Results.....	8
3.1 2D spline correction.....	9
3.2 Camera projection.....	10
4 Applications.....	11
Appendix.....	12
Determination of zenith coordinates.....	12
Simple model fit.....	13
Full model fit and image overlay.....	14

Version history

Version	Date	Section	Change Description
1	2023-06-06	all	

List of figures

Figure 1: All-sky camera installed in its temporary testing position at Yebes.....	ix
Figure 2: Characteristics of the sensor mounted in the all-sky camera. ASI website [2].....	2
Figure 3: Flow diagram of the astrometric calibration procedure implemented for this work.....	6
Figure 4: Example of a night image taken with the all-sky camera at Yebes Observatory (left) and an overlay of the sources detected by the extraction software (right).....	7
Figure 5: Star position residuals from a single frame calibration.....	8
Figure 6: Star position residuals obtained from stacking 27 frames.....	8
Figure 7: Star position residuals. 50 frames, no 2D spline correction.....	9
Figure 8: Star position residuals. 50 frames, with 2D spline correction.....	9
Figure 9: Instantaneous field of view (IFOV), or angle subtended by a single pixel. Near the horizon the resolution is worse than at the zenith.....	10
Figure 10: Example of the determination of zenith coordinates by meridian crossings.....	12
Figure 11: Astrometric calibration performed with a simple 5-parameter model.....	13
Figure 12: Overlay of compass directions and azimuthal grid over a calibrated image.....	14

Abbreviations

ADS-B	Automatic Dependent Surveillance-Broadcast
FITS	Flexible Image Transport System
RMS	Root Mean Square
SLR	Satellite Laser Ranging
YDALGO	Infraestructuras de desarrollo de laboratorio para geodesia espacial en el Observatorio de Yebes
YLARA	Yebes Laser Ranging

Applicable and reference documents

References

- [1] [ZWO ASI294MC Pro](#) (ZWO website, last retrieved 30/05/2023)
- [2] García Marín et al. YLARA Sensors Installation and Outdoor Tests. [CDT Technical Report 2022-6](#), 2022.
- [3] Borovička et al. A new positional astrometric method for all-sky cameras. *Astron. Astrophys. Suppl. Ser.* 112, 173–178, 1995
- [4] Barghini et al. Astrometric calibration for all-sky cameras revisited. *Astron. Astrophys.* 626, A105, 2019
- [5] Bertin, E. & Arnouts, S. 1996: SExtractor: Software for source extraction, *Astronomy & Astrophysics Supplement* 317, 393.
<https://www.astromatic.net/software/sextractor>
- [6] Rhodes, B. Skyfield: High precision research-grade positions for planets and Earth satellites generator. *Astrophysics Source Code Library*, 1907.024. 2019.
<https://ui.adsabs.harvard.edu/abs/2019ascl.soft07024R>

Abstract

All-sky cameras are a staple of astronomical and SLR observatories. They are normally employed as environmental awareness tools, showing cloud presence, illumination conditions, and the laser beam direction. For actual positional tasks requiring certain degree of accuracy, these cameras require a star calibration to correct for their physical orientation, internal misalignments, and the optical behaviour of the lenses. This accomplished, they become precise measuring instruments that can find new uses. We have performed the astrometric calibration of the all-sky camera that will be used for supporting SLR operations at Yebes Observatory, achieving sub-pixel positional precision and thus enabling several applications beyond mere situational awareness.



Figure 1: All-sky camera installed in its temporary testing position at Yebes.

1 Introduction

For the new satellite laser ranging station at the Yebes Observatory (Guadalajara, Spain), an all-sky camera was purchased to aid observers in their operations. All-sky, or whole sky cameras, employ a fisheye lense to achieve very large fields of view, often covering the whole horizon. The primary function of these instruments in SLR stations is environmental awareness for system operators, e.g. detecting the presence and position of clouds, assessing the illumination conditions, the positions of the Sun and the Moon, and that of the laser beam. Due to the limited angular resolution and often moderate sensitivity of these cameras, their use for air safety purposes is at best secondary. Still, provided that a suitable calibration is performed, they can complement other safety systems with independent positional information that could be employed either operationally or for analysis and validation purposes.

The astrometric calibration of these optical systems has been researched for meteor astrometry, where positional measurements of the same atmospheric entry event by geographically distributed cameras are used for orbit determination. Several observational networks are currently deployed internationally for this purpose, employing different hardware setups but relying on the same principle.

We have implemented a calibration system for our camera following a selection of methods described in the literature, achieving sub-pixel positional precision (<2 arcmin RMS in Az/EI). The calibration system requires no manual intervention after an initial coarse setup, and includes the steps of source extraction, selection, matching, and least squares fit of the camera model. A fully calibrated all-sky camera allows for pixel-perfect accurate overlays (e.g. in operational graphical user interfaces with predicted satellites or aircraft positions relayed by ADS-B) as well as their use for meteor observations within dedicated networks. It also makes feasible to employ these cameras for complementary safety purposes.

2 Implementation

2.1 Hardware

The all-sky camera we employed for this work is an OMEA-8C, manufactured by Alcor System. Internally, this device uses a ZWO ASI294MC Pro camera [1], which combined with the optics mounted in the OMEA-8C package, provides a usable resolution of $\sim 2800 \times 2800$ pixels, with an instantaneous field of view slightly larger than 4 arcmin. The ZWO camera has a back-illuminated Sony sensor IMX294CJK, whose main features are shown in Figure 2.

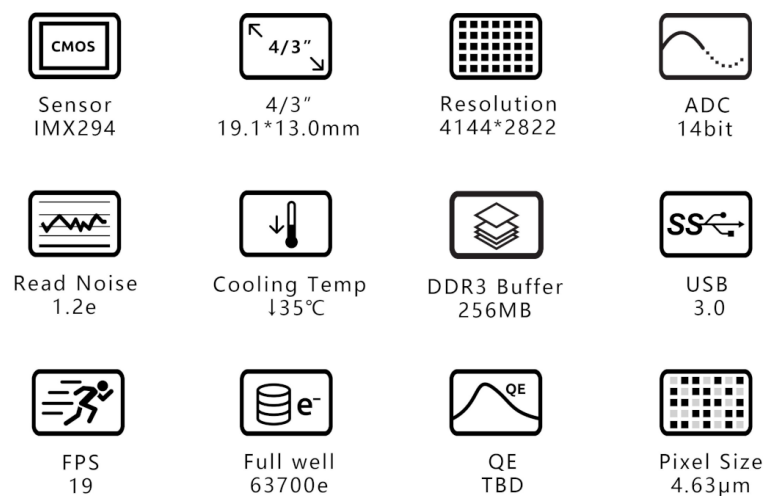


Figure 2: Characteristics of the sensor mounted in the all-sky camera. ASI website [2].

Over a period of several months in 2021, we collected night sky images exploring different settings [2], employing the software included with the camera (Windows OS only). This proved rather unreliable, limiting, and frustrating due to software limitations and frequent communication problems between the control PC and the device. The integration of the camera at the station will involve direct communication with the ZWO camera instead of using the software provided by Alcor System, which will provide greater flexibility in its operation.

2.2 Calibration model

The astrometric calibration of an all-sky camera is conceptually identical to the determination of a pointing model for a telescope mount. The encoder positions of the two axes of the mount are equivalent to the pixel positions of the images taken with the camera. The problem consists in the determination of the optimal parameters of a model that relates the instrumental coordinates (pixel or encoder positions) to sky coordinates. Of course, the specific mathematical form of the models em-

ployed for cameras or telescope mounts are very different, for they relate and correct for completely different physical effects.

Thus, camera models must take into account the inevitable imperfect orientation of the device in the horizontal and vertical planes, the misalignment of the optical axis, the specific optical projection of the lense and associated distortions, and the possible misalignment of the internal sensor relative to the optical axis.

Methods and solutions to the problem of calibrating cameras with ultra wide fields of view, which include all-sky cameras, can be found in the literature of the fields of computer vision and astronomy. The procedures followed in the computer vision domain usually involve the imaging of regular patterns (e.g. high contrast square grids) that are used to extract the camera parameters. The approach in the astronomical literature is to employ images of star fields, which are then extracted as the reference sources for the calibration, estimating both the model parameters related to the instrument as well as its absolute orientation in space.

A popular model in meteor astronomy was given by Borovička et al 1995 [3], with several improvements published since first proposed. More recently, Barghini et al 2019 [4] reformulated some of the expressions, which together with a slightly modified strategy led to improvements in the estimability of the model parameters. Our implementation adopts features from both approaches, using the updated expressions from Barghini et al 2019, but including the azimuthal correction present in Borovička 1995 to improve the model fit, and finally adding a 2D spline empirical correction to further reduce the post-fit residuals.

The expressions of the implemented model follow, but interested readers are encouraged to consult the references given to grasp the mechanics of the model and the geometrical meaning of the variables:

$$r_\epsilon = \sqrt{(x_0 - x_z)^2 + (y_0 - y_z)^2}$$

$$E = a_0 + \arctan\left(\frac{y_0 - y_z}{x_0 - x_z}\right)$$

$$\epsilon = V r_\epsilon + S(e^{Dr_\epsilon} - 1),$$

where

x_0, y_0 : plate coordinates of the optical axis

x_z, y_z : plate coordinates of the zenith

E, ϵ : distance between the optical centre and the zenith

a_0 : complement of angular offset relative to the North direction

These three expressions are the new parameterisation of the model given by Barghini et al 2019, which improve the estimability of the solution and allows for the determination of the zenith coordinates directly. Additionally, with the zenith coordinates explicitly included in the expressions, it is possible to determine the zenith position independently and reintroduce its coordinates in the

model (Barghini et al propose the method of meridian crossings, interpolating stellar trajectories over the crossing of the local meridian, see appendix). This approach may be useful in certain cases, such as in the initialisation stages of the model fit and for low-resolution systems, which present a high sensitivity to the starting points. At model initialisation it is likely that suitable initial guesses for the model parameters are not available, incomplete, or guessed with only very limited accuracy, therefore possibly compromising the convergence of the least squares fit. Outside these situations, we have found that it is perfectly feasible to estimate x_z, y_z along with the rest of the parameters, without noticeable loss of precision or any otherwise undesirable behaviour.

The following relations complete the model:

$$r = \sqrt{(x - x_0)^2 + (y - y_0)^2} + A(y - y_0) \cos(F - a_0) - A(x - x_0) \sin(F - a_0)$$

$$b = a_0 - E + \arctan\left(\frac{y - y_0}{x - x_0}\right)$$

$$u = Vr + S(e^{Dr} - 1),$$

where

r : distance to the optical centre, which includes an added term to remove azimuth-dependent scale variations (see Borovička [4]), with estimated parameters A and F

b, u : angular distances relating plate coordinates and projection coordinates in azimuth and zenith distance, respectively

a_0 : complement of angular offset of the image with respect to the North direction

Finally, the expressions for azimuth and zenith distance are:

$$Az = E + \arctan\left(\frac{\sin u \sin b}{\sin u \cos b \cos \epsilon + \cos u \sin \epsilon}\right)$$

$$Zd = \arccos(\cos u \cos \epsilon - \sin u \sin \epsilon \cos b).$$

Thus, we have to estimate the plate constants a_0, x_0, y_0 ; the camera constants A, F ; the lens constants V, S, D ; and the station constants ϵ, E . As mentioned, the coordinates of the zenith may be co-estimated with the rest of parameters or determined directly through e.g. the observation of meridian crossings (see appendix).

In addition to this set of parameters, we added an empirical correction to the solution, consisting in a 2D-spline fitted to the post-fit residuals in azimuth and elevation resulting from the use of the model above. The reason for this additional correction is that, after performing multiple calibrations accumulating a large number of frames, we noticed that the residuals presented a complex pattern, at the level of ~ 2 arcmin, which could not be removed via the introduction of additional parameters. We found that this pattern was quite stable throughout time, presenting no change when observations from different nights were employed, and therefore concluded that it reflects some physical characteristics of the camera/lens. Fitting to the residuals the surface given by a 2D-

spline successfully removes this pattern almost entirely, improving the final RMS of fit to approximately 1 arcmin.

The system of equations can be solved by univariate least squares, stacking the coordinates side by side, and can be written in matrix form as $XB = Y$, where

X : partial derivatives of Az, Zd

B : vector of parameters

Y : residuals in $Az \sin Zd$ and Zd

2.3 Strategy

There are several difficulties and pitfalls to be aware of in order to perform the astrometric calibration successfully:

- Highly non-linear model
- Very sensitive to the initial conditions
- Analytical Jacobian exists but is too cumbersome for practical use
- Initial parameter guesses mostly unknown

A consequence of these is that the initial setup of the system, with reasonable values for the solve-for parameters, require an iteration process with manual intervention, and possibly the use of a simplified model until stable convergence is achieved, as it was our case.

The partial derivatives of the model with respect to the parameters can be derived with the help of any computer algebra system. However, we found the resulting expressions to be too unwieldy to be used, and therefore we computed them numerically instead. In so doing one must make sure that the approximations are adequate and that suitable methods are employed, so that convergence is not affected.

Once a preliminary model is obtained, with coarse values for the model parameters, the calibration process can be streamlined and performed without user intervention. For the automation of the source extraction we have used the software SExtractor [5], and for the computation of stars visibility and positions the Python library Skyfield [6]. The least squares solver and the main program driving the whole process we implemented in Python, using the libraries Numpy, SciPy and Pandas.

The structure of the implementation of the astrometric calibration is the usual two-branch process adopted in many parameter estimation problems, as shown in the diagram in Figure 3. The observations, consisting in one or more sky frames taken with the camera, are processed with SExtractor to detect and extract the sources of interest. The sources are filtered using criteria based on shape parameters obtained with SExtractor, such as elongation, absolute size, and SExtractor star classification. At that point, the currently available model for the transformation of instrumental to celestial coordinates is used to obtain the positions of the filtered sources in the celestial frame.

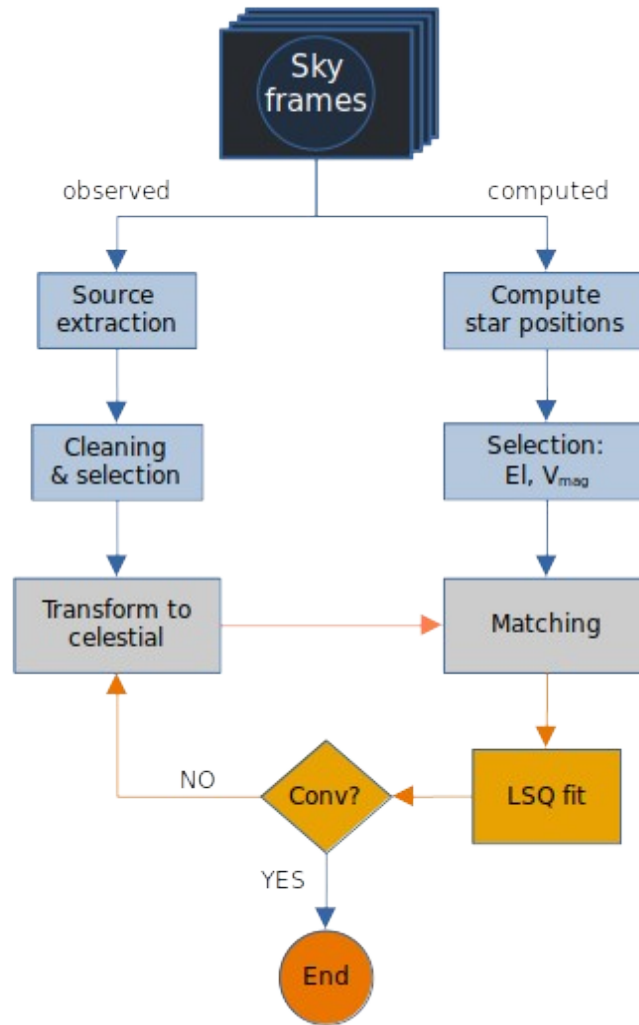


Figure 3: Flow diagram of the astrometric calibration procedure implemented for this work.

In the so-called computed branch, the epoch of the observations is read from the header of the FITS files, which together with the geographical coordinates of the site are used to compute the ephemerides of stars visible from the observatory at that time. The visible stars are filtered on the basis of minimum elevation and magnitude before proceeding with the comparison with the empirically detected sources. For this, the computed positions from the star catalogue have to be matched to source positions, which in our implementation we perform in the sky frame. The matching step is achieved computing the pairwise great circle distances with the haversine formula, identifying the sources with the stars with minimum distance. This may occasionally lead to incorrect source identification if the transformation to celestial coordinates in the current iteration is of low quality, something which can be easily avoided by starting the fitting process with a restrictive magnitude threshold, therefore limiting the number of possible matching stars to the few brightest ones. As the model improves, the threshold can be relaxed and the source matching performed with a greater number of stars, so that most sources detected are utilised and contribute to the fit.

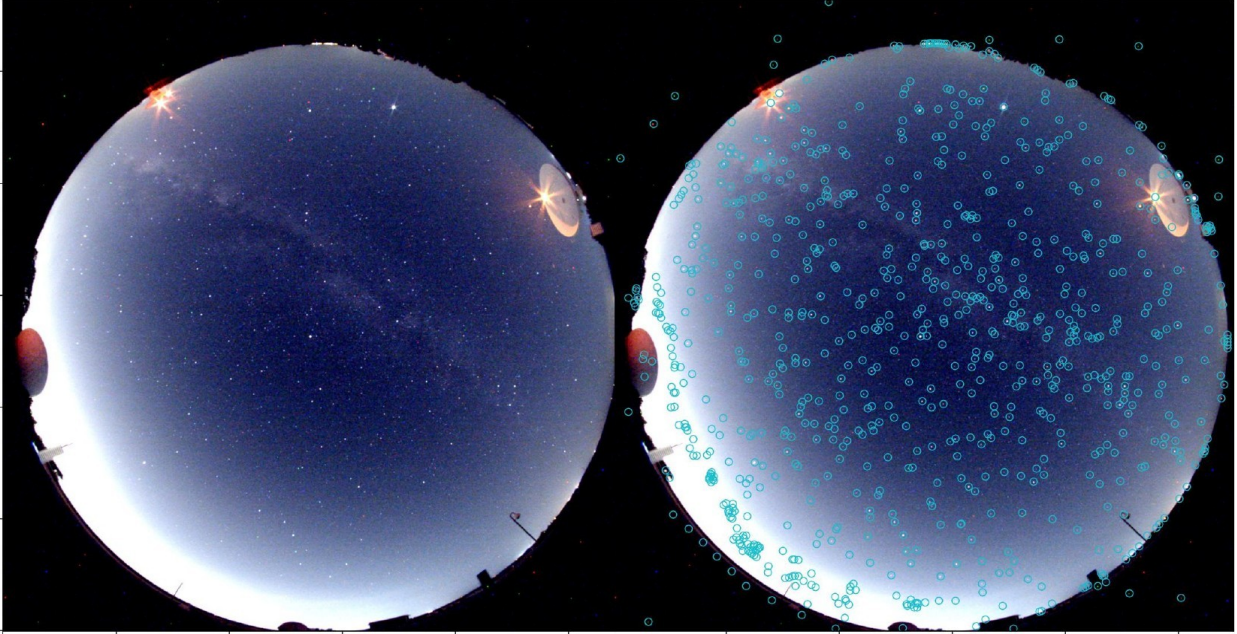


Figure 4: Example of a night image taken with the all-sky camera at Yebes Observatory (left) and an overlay of the sources detected by the extraction software (right).

The iterative loop of parameter estimation, coordinates transformation and source matching is continued until some convergence criteria is met, such as certain threshold for percentage reduction in the variance of unit weight between iterations and/or maximum number of iterations.

In a typical frame of the cloudless sky at Yebes, about 500 star sources can easily be extracted and matched with an elevation cut-off of 20 degrees and a limiting visual magnitude of 6.5. Figure 4 shows a 45-seconds exposure taken from the temporary testing location of the camera, and the 838 sources extracted by SExtractor. Of these, 475 were successfully matched to the predicted positions of the 3114 stars visible at that instant within the elevation and brightness threshold limits. It is inevitable that some of the sources detected are spurious, such as artificial lights or excessively bright regions in the image towards the horizon, as can be appreciated in the figure. Nonetheless this does not affect the calibration process as these sources are rejected at the star matching stage.

3 Results

We have tested the implemented calibration procedure with single frames of different exposure times, from 10–45 seconds. All exposure times are satisfactory, although the star magnitude and therefore the number of sources available obviously decrease with exposure time. It is also feasible to accumulate the sources extracted from different frames, and perform the calibration with a very large number of observations that ensures a virtually perfect coverage of the celestial hemisphere. This accumulation of multiple frames taken over several hours is a necessity to estimate the empirical correction to remove certain patterns in the residuals.

Examples of the post-fit residuals, in polar projection and in azimuth and elevation, obtained with a single frame (459 sources extracted) and after accumulating 27 frames collected throughout a single night (12400 sources) are shown in Figure 5 and Figure 6. The RMS of the fit is about 1 minute of arc, which is ~ 4 times lower than the pixel field of view of the camera, therefore achieving sub-pixel positional precision. Typical estimated values obtained are given in the appendix.

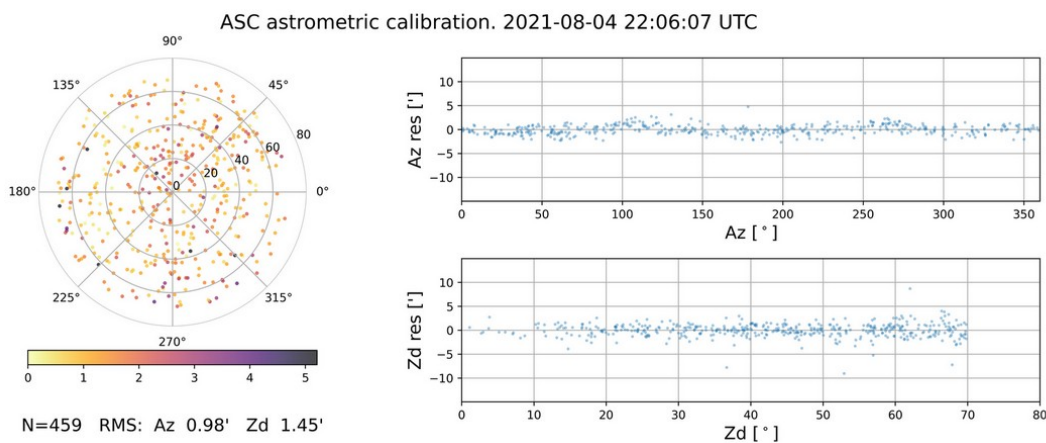


Figure 5: Star position residuals from a single frame calibration.

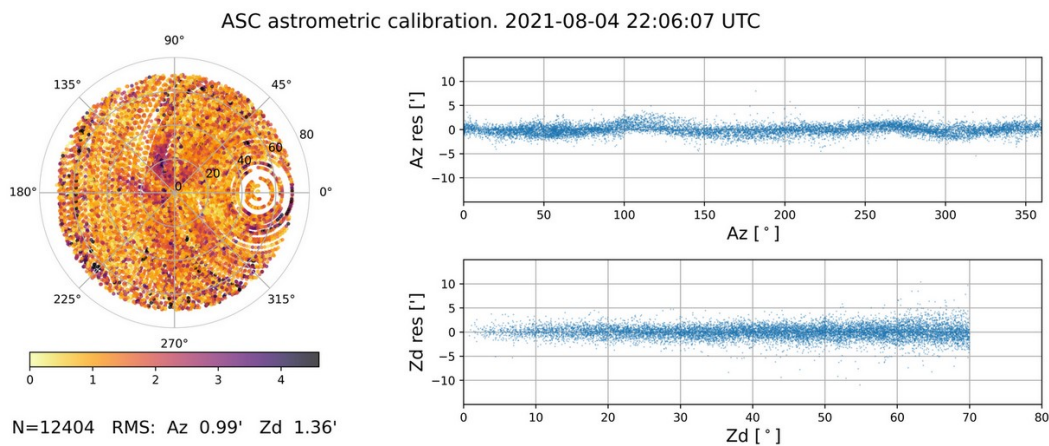


Figure 6: Star position residuals obtained from stacking 27 frames.

The quality of the calibration is maintained at all elevations, which is notable for these camera devices, whose optical projection and associated distortions are most conspicuous and difficult to model at large zenith distances close to the horizon.

3.1 2D spline correction

To illustrate the effect of the correction applied in addition to the model described in the previous section, the geometry and magnitude of the post-fit residuals obtained with and without the 2D spline is shown in Figures 7 and 8. Without this correction the presence of a complex pattern is clearly present in the residuals, with deviations over 5 arcmin in some regions. Fitting a surface in azimuth and elevation to the residuals provides a correction that can be afterwards applied during the iterative calculation of the solution, so that the estimated parameters are not forced to fit these features. With this strategy, the pattern in the residuals is almost completely removed, and the precision of the solution is improved significantly.

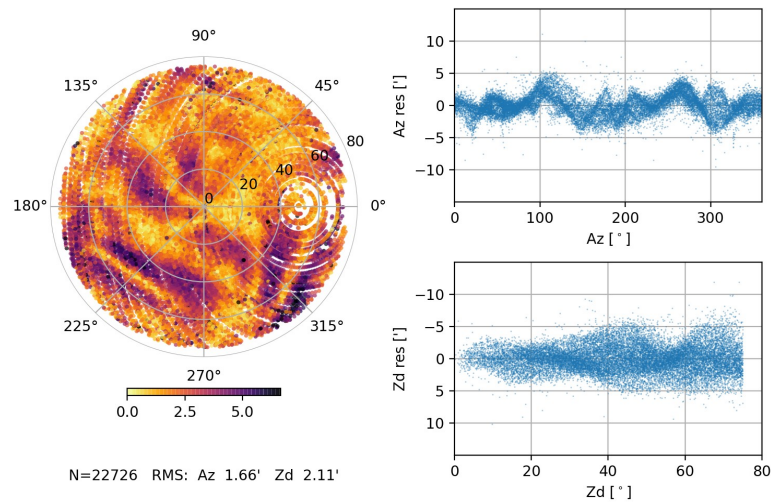


Figure 7: Star position residuals. 50 frames, no 2D spline correction.

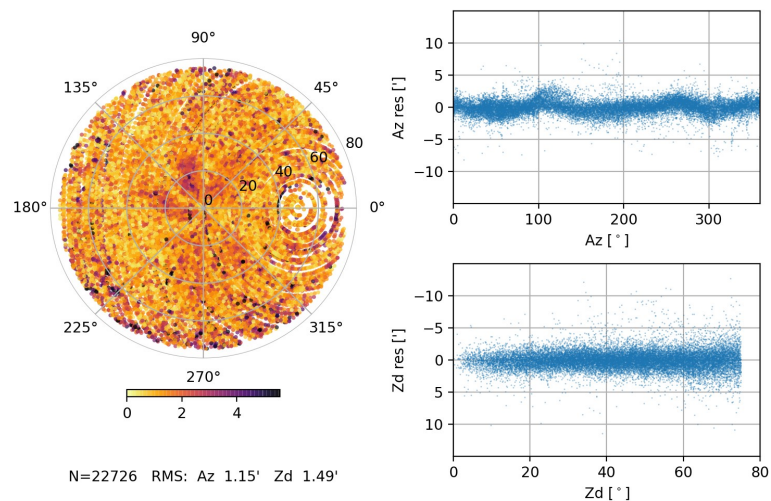


Figure 8: Star position residuals. 50 frames, with 2D spline correction.

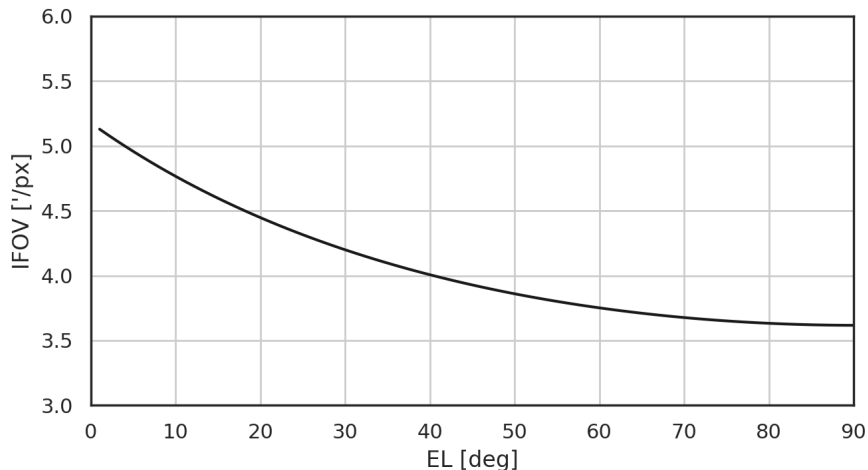


Figure 9: Instantaneous field of view (IFOV), or angle subtended by a single pixel. Near the horizon the resolution is worse than at the zenith.

However, it must be noted that even without applying the additional spline correction, the positional errors obtained are comparable to the resolution of the camera, which average 4 arcmin approximately (see Figure 9). The best precisions achieved with the model plus post-fit corrections are close to 1 arcmin, and thus we can speak of sub-pixel positional resolution of the camera calibration. This is possible thanks to the fact that the sources extracted for the calibration have positions whose precisions are better than a single pixel, since they are computed by SExtractor as weighted averages of their pixel values.

3.2 Camera projection

The model described in section 2.2 was the one chosen out of several models explored, as it was the most performant one in terms of final RMS of fit. In the first stages of the solving procedure we employed the simplified model given by Barghini [4] to obtain a convergent solution for the initial star matching step. It was thus realised that the camera lense can be approximated very well by an equisolid fisheye projection with a centre offset, which could be said to be the designed projection of the camera. The expressions for the celestial to pixel coordinates transformation of this projection are given here [2]:

$$x = x_c + r_c \cos(Az - a_0)$$

$$y = y_c + r_c \sin(Az - a_0)$$

Although the precision achieved with this model is about 4 times worse than that obtained in the more complex solution (5 estimated parameters vs 10, see appendix), it is nonetheless useful as it has a very simple analytical inversion, which the complex model lacks. Thus, where the utmost achievable precision is not required, this model is convenient, in particular for the inverse transformation.

4 Applications

The positional alignment of the images obtained with all-sky cameras is usually performed only coarsely, if at all. This is acceptable for some of the operational uses of these devices (e.g. operator sky awareness). In richer applications, the sky images can be augmented with graphic overlays that include items such as the positions of aircraft detected by ADS-B, satellite orbits, stars, and the celestial grids (see appendix for an example). The quality of this kind of user interfaces benefits from the availability of positional precisions at or near the pixel level.

Beyond the mere display of information over sky images, astrometrically calibrated cameras could be employed for air safety purposes. A possible application in this regard is the validation of positional data obtained through other methods, such as FLARM, ADS-B, or other cameras. In principle, calibrated all-sky cameras could be used as a safety tool on their own right, complementing other existing instruments¹.

Applications outside the field of SLR include the integration of calibrated devices in meteor sensing networks, which employ the positional data collected simultaneously by several cameras geographically distributed to calculate the trajectories of meteors in the upper layers of the atmosphere.

The implementation of the astrometric calibration, with its identification of sources from star catalogues, allows with little additional effort the computation of a photometric calibration, since the magnitudes of the matched stars are automatically available, as well as the photometric information from the extracted sources. This opens up the possibility to employ the camera as a sky quality monitor, and its comparison with dedicated devices for this purpose. Initial testing of this possibility seems promising, and should be further explored.

¹ A preliminary study of this topic is underway, with the exploration of methods to extract the positions of aircraft from all-sky images, and their comparison with ADS-B positions.

Appendix

Determination of zenith coordinates

As explained in Barghini et al 2019 [3], their formulation allows for the inclusion of an independently determined pair of coordinates for the zenith position in the camera images. A method to accomplish this is through the analysis of the meridian crossings of stars. Stars in the data set that cross the meridian are selected. The precise time of culmination is computed from the series of images and then the pixel coordinates are interpolated. Plotting these data in x and y against declination, as shown in Figure 10, allows for the direct determination of the zenith coordinates, which correspond to the intersection of these lines with the declination corresponding to the latitude of the site.

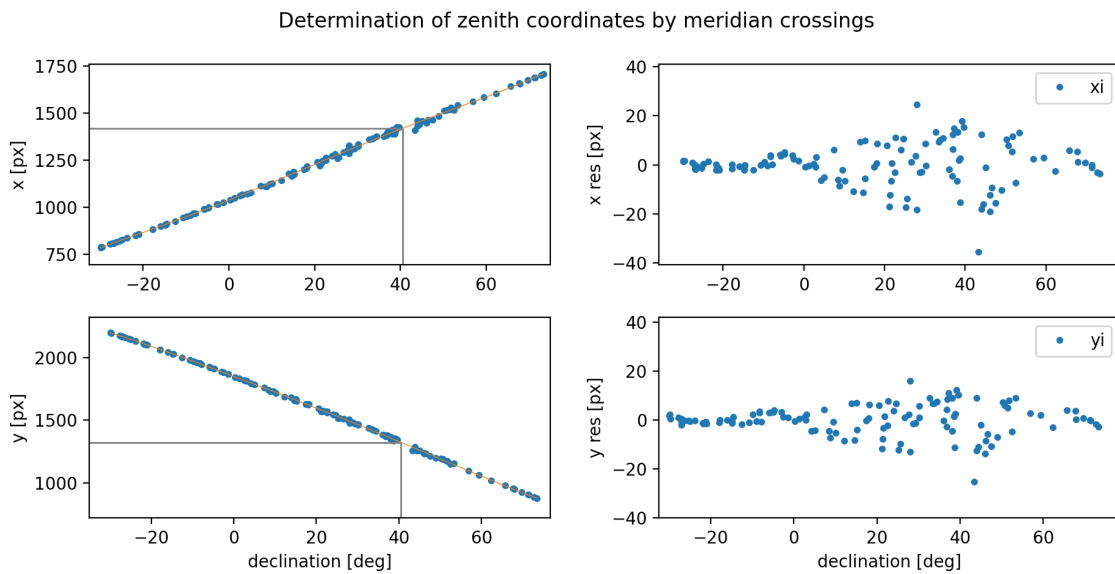


Figure 10: Example of the determination of zenith coordinates by meridian crossings.

Simple model fit

The overall precision achieved with the simple 5-parameter model, as measured by the post-fit RMS, is about 4 times worse than that obtained with the full solution. There appear evident features in the position residuals in azimuth and elevation that indicate the inability of this simplified model to account for the behaviour of the camera system (Figure 11). It is however a very useful model for the initial stages of the calibration process, and for the inverse transformation (celestial to instrumental coordinates).

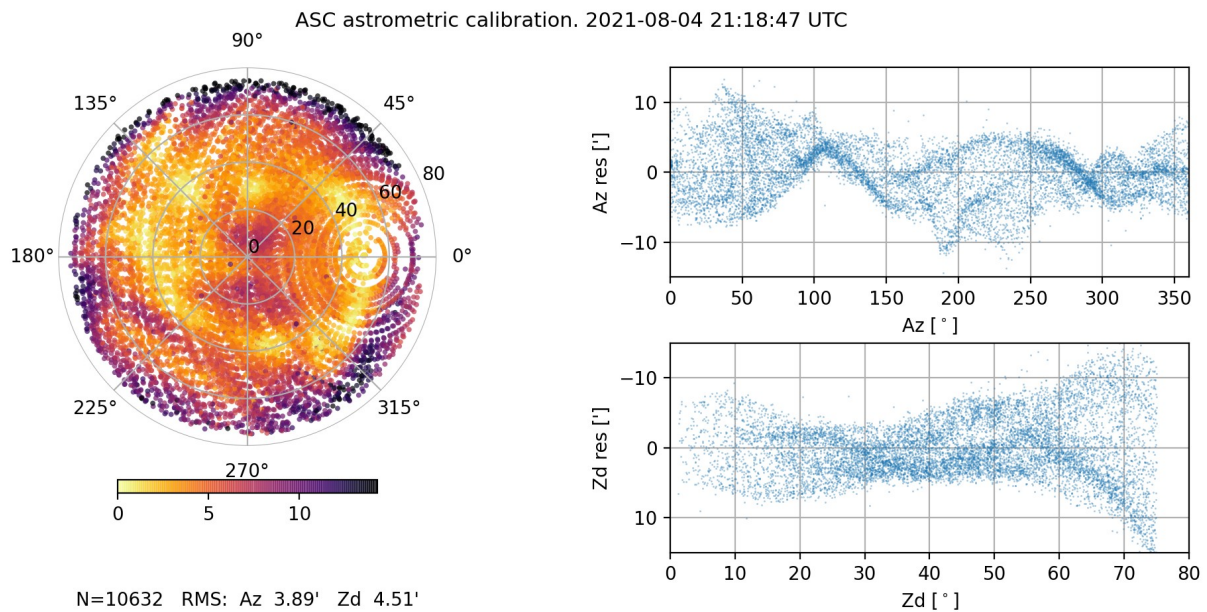


Figure 11: Astrometric calibration performed with a simple 5-parameter model.

Full model fit and image overlay

The values of the set of estimated parameters from a calibration run using the full 10-parameter model are provided below as an example. The horizontal offset of the camera image relative to the North direction has been estimated as 34.54 degrees (complement of a_0). The compass directions and an azimuthal grid at 5, 15, 30, 45, 60 and 75 degrees are shown in Figure 12. Any position in the image can be readily transformed to celestial coordinates with pixel precision, and the inverse transformation used to display positions on the image, as in this example.

```

a0=0.968 [rad]
x0=1400.2, y0=1307.6 [px]
xz=1403.6, yz=1314.5 [px]
A=-2.1e-3, F=3.3
V=1.1e-3, S=5.8e-3, D=2.7e-3

```

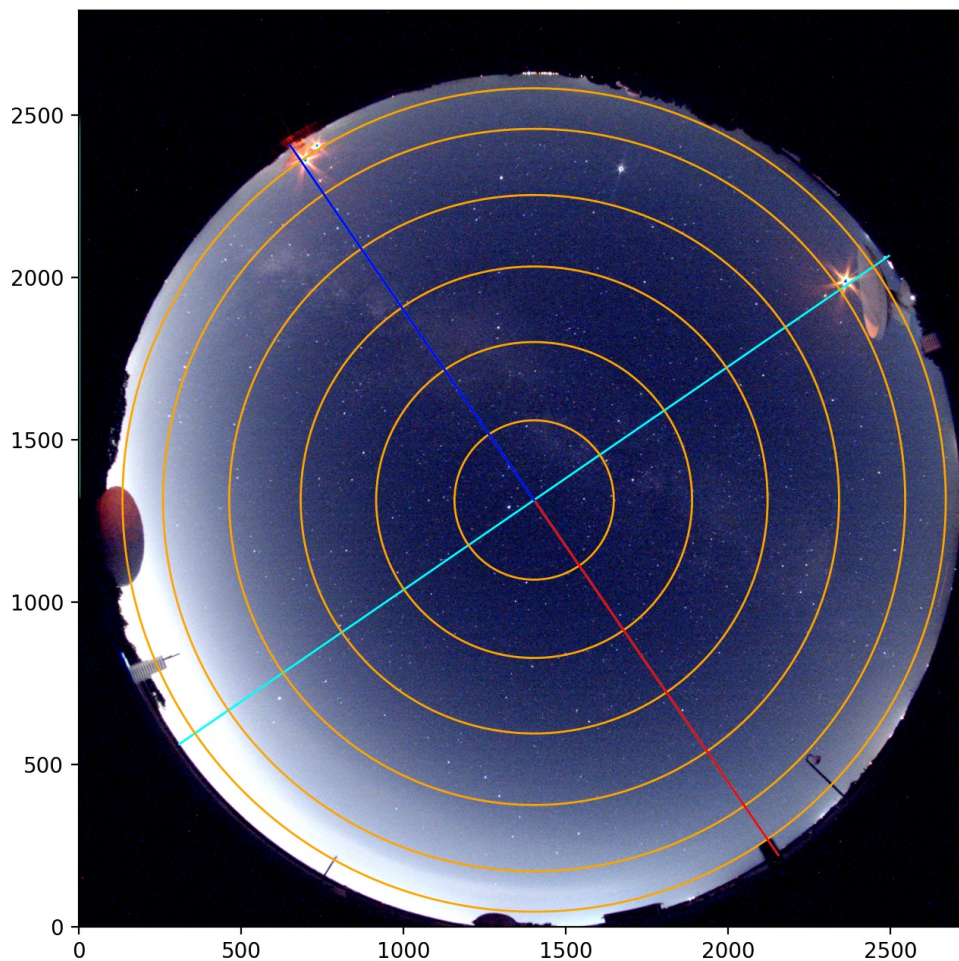


Figure 12: Overlay of compass directions and azimuthal grid over a calibrated image.

Astrometric calibration of Yebes all-sky camera
Yebes Observatory, June 2023